MRD-CI Characterization of Electronic Spectra of Isoelectronic Species C_6^-, NC_4N^+, and CNC_3N^+

Zexing Cao[†] and Sigrid D. Peyerimhoff*[,‡]

Institut für Physikalische und Theoretische Chemie, Universität Bonn, Wegelerstrasse 12, D-53115 Bonn, Germany, and Department of Chemistry, State Key Laboratory for Physical Chemistry of the Solid Surface, Xiamen University, Xiamen 361005, China

Received: July 26, 2000; In Final Form: November 3, 2000

The structure and stabilities of linear and cyclic isomers of C_6^- and $N_2C_4^+$ were investigated by DFT, MP2, CISD, and CCSD methods. The linear isomers of C_6^- and NC_4N^+ are predicted to be the most stable forms. Multireference configuration interaction methodology was used for the calculation of the doublet and quartet excited states. Assignments to observed transitions in matrix spectroscopy of these species are made. The first X $^2\Pi \rightarrow {}^2\Pi$ transitions for C_6^-, NC_4N^+, and CNC_3N^+ occur at 1.98, 2.14, and 2.65 eV, respectively, showing similar features with large oscillator strengths. On the other hand, a significant difference exists in the X $^2\Pi_u \rightarrow 1\ ^2\Sigma_g^+$ band system between the C_6^- and NC_4N^+. Correlation between the relative molecular orbital energy and spectroscopic properties is discussed. The predicted electronic spectra agree well with available experimental data.

Introduction

New developments in matrix isolation spectroscopy have led to spectroscopic characterization of mass-selected carbon clusters in the gas phase.[1] A number of absorption bands of carbon chains and their derivatives were found to match the diffuse interstellar bands (DIBs), showing that these carbon clusters are possible candidates for the carriers.[2−5] Among the numerous transitions observed, only a few bands of specific species were assigned, both experimentally and theoretically.[6−8] A precise understanding of these electronic spectra remains open.

Small carbon chains were proposed as good candidates for DIBs by Douglas.[9] Furthermore, the existence of cyanopolyacetylenes in dark interstellar clouds is well-known experimentally.[10] These small carbon chains and nitrogen-containing chains bear the electronic structure and the bonding feature of extended π conjugated systems. Therefore, they serve as ideal models for exploring larger carbon clusters theoretically. The structure and stabilities of small carbon clusters (up to 10 carbon atoms) have been studied by sophisticated theoretical calculations, and the results are discussed in connection with experimental findings in the recent reviews of Orden and Saykally[11] and Weltner and Van Zee.[12] However, the low-lying excited states of carbon chain anions and cations have received much less attention.

Previous theoretical calculations[13−15] have characterized the $^2\Pi_u$ ground state and several low-lying excited states of linear C_6^-. A RCCSD(T) study by Schmatz and Botschwina[13] predicts that transitions X $^2\Pi_u \rightarrow$ A $^2\Sigma_g^+$ and X $^2\Pi_u \rightarrow$ B $^2\Pi_g$ occur at 1.313 and 2.120 eV,[13] which are close to the corresponding bands of 1.16 and 2.04 eV observed by Maier and co-workers in neon matrix.[16,17] For higher excited states, there is a significant discrepancy between experiment[17] and CIS[18] and UHF/FOCO/CCSD methodologies.[14] Furthermore, there still are inconsistencies among theoretical results.[13,14,18]

C_6^- and NC_4N^+ are isoelectronic species. Their X $^2\Pi_u \rightarrow {}^2\Pi_g$ band systems appear in a similar region, i.e., at 2.04 eV[16] in C_6^- and at 2.07 eV[19] in NC_4N^+. However, significant differences exist for other bands. For example, the X $^2\Pi_u \rightarrow 1\ ^2\Sigma_g^+$ band of C_6^- centers at 1.16 eV,[17] while this transition occurs at 2.16 eV for the NC_4N^+ species.[19] Similar differences can be found between other bands of C_6^- and NC_4N^+. For NC_4N^+ species, no *ab initio* calculation on electronically excited states is available so far.

Although tentative assignments of several bands for these species have been made, a definite assignment is difficult due to the uncertainty resulting from the concomitant presence of several compounds in the observed spectra as well as the lack of theoretical support. Extended theoretical studies are required to clarify these assignments. For this reason, an *ab initio* study on the excited states of C_6^-, NC_4N^+, and CNC_3N^+ will be presented in this work. Electronic spectra due to doublet excited states of these species are determined by using a multireference configuration interaction method (MRD-CI). Theoretical predictions for the quartet system of C_6^- will be made as well.

Computational Details

In the MRD-CI calculation, the basis set used in this study is the 9s5p/5s3p Gaussian set[20] for all atoms augmented with one d-polarization function (exponent 0.75) on each atom. Such basis is known to possess sufficient flexibility in describing a series of electronically excited states in a balanced manner; it is preferred over a larger basis set optimized for ground-state properties. A 2p anionic function (exponent 0.034), an *s*-type diffuse function (exponent 0.0438), and a 3p Rydberg function (exponent 0.021) are included for the C_6^- anion.[21] For dicyanoacetylene cations, Rydberg functions 3s (exponents 0.023 for C and 0.028 for N) and 3p (exponents 0.021 for C and 0.025 for N) are added to the double-ζ plus polarization basis set.[21]

* Corresponding author. E-mail: unt000@uni-bonn.de. Fax: +49-228-739064.
[†] Xiamen University.
[‡] Universität Bonn.

10.1021/jp002659x CCC: $20.00
Published on Web 01/03/2001

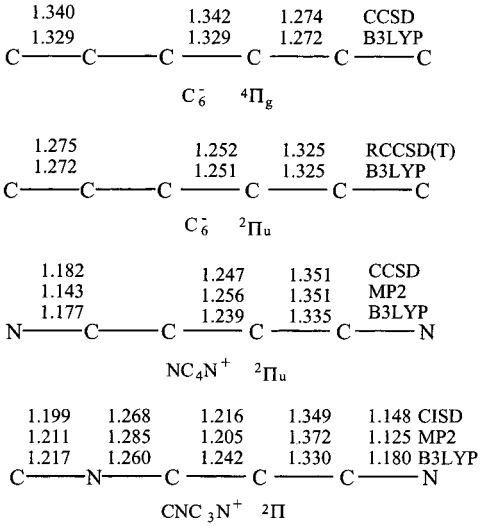

Figure 1. Optimized geometries of C_6^-, NC_4N^+, and CNC_3N^+ linear chains at different levels of sophistication.

For all DFT(B3LYP), MP2, CISD, and CCSD calculations, the basis set has a quality of 6-311G*.[22,23]

Density functional calculations with the B3LYP functional were used to determine the equilibrium geometries and vibrational frequencies of the ground states. The geometry of selected states was optimized in addition by MP2, CISD, and CCSD methods. In subsequent MRD-CI calculation, the MRD-CI multireference configuration interaction procedure based on general configuration selection and perturbation estimates[24] was used. The MOs used for MRD-CI calculations were from CASSCF optimization. All calculations were carried out with Gaussian 94,[25] MOLCAS version 4.0,[26] and DIESEL-CI programs.[27]

MRD-CI calculations, including all 25 valence electrons and 21 partial valence electrons, respectively, yield almost the same results, showing that inner 4 valence electrons can be reasonably deleted from the active reference space. The highest 12 MOs were deleted so that 21 electrons were allowed to be distributed among 136 MOs for C_6^- and 118 MOs for NC_4N^+ and CNC_3N^+ in the MRD-CI. The configuration selection thresholds were generally 10^{-7} and 5×10^{-8} hartree. The extrapolation to the full MRD-CI space was carried out in the standard manner. The generalized Davidson procedure was used to recover contributions from higher excitations. This extrapolated full CI limit with Davidson's correction will be used throughout in the present study.

The corrected RCCSD(T) optimized geometry of the ground-state C_6^- from ref 13, the DFT(B3LYP) optimized geometry of CNC_3N^+, and the CCSD optimized geometries of the ground state of NC_4N^+ and the quartet state of C_6^- were used in the MRD-CI calculation (Figure 1). For the ground state and the quartet state of C_6^-, DFT calculations predicted excellent geometries in comparison with the corrected RCCSD(T) and CCSD optimized geometries, as will be discussed later.

Results and Discussion

Geometries and Stabilities. The calculations to obtain the optimal geometry for cyclic and linear isomers of C_6^-, NC_4N^+, and CNC_3N^+ in their ground states as well as the zero point frequencies have been performed by the DFT(B3LYP) approach. For comparison, geometries of relevant linear stable species have been reoptimized by MP2, CISD, and CCSD methods. Figure 1 presents the optimized geometries at different levels of theory.

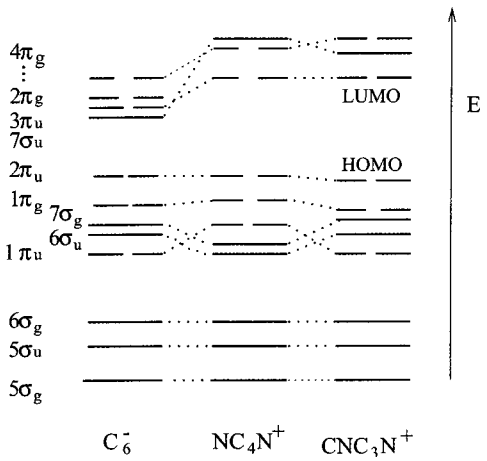

Figure 2. Molecular orbital relative energies of C_6^-, NC_4N^+, and CNC_3N^+.

The geometries of NC_4N^+ and CNC_3N^+ in Figure 1 show an acetylenic character for NC_4N^+ while prominent cumulenic bonding for CNC_3N^+, i.e., N≡C−C≡C−C≡N$^+$ and C═N═C═C−C≡N$^+$. Other possible isomers for dicyanoacetylene cations and C_6^- were investgated. The NC_4N^+ linear arrangement of atoms is found to be lowest in energy, followed by the corresponding linear CNC_3N^+ arrangement. NC_4N^+ ($^2\Pi_u$) is lower in energy than CNC_3N^+ ($^2\Pi$) by 15.8, 19.2, and 16.2 kcal/mol at the B3LYP, MP2, and CCSD levels of treatment. The lowest $^2A_1$ state of a cyclic isomer in C_{2V} symmetry (similar to a distorted structure of D_{3h} symmetry) is higher than the NC_4N^+ ($^2\Pi_u$) by 62.7 kcal/mol at the B3LYP level. Similarly, the $^2A_1'$ state in D_{3h} symmetry of the C_6^- ring lies 40 kcal/mol above the X $^2\Pi_u$ lowest state of linear C_6^-. This situation differs from the case of C_6^+, for which the linear and ring isomers are basically isoenergetic. The CCSD calculations predicted that the quartet state $^4\Pi_g$ of C_6^- is above the doublet ground state $^2\Pi_u$ by 48.5 kcal/mol after zero-point vibrational energy correction.

Table 1 presents harmonic vibrational frequencies of species C_6^-, NC_4N^+, and CNC_3N^+ at the B3LYP level. The strongest vibrational band $\upsilon_4(\sigma_u^+)$ of C_6^- was predicted to lie at 1939 (2026) cm^{-1}. A comparison of calculated and experimental values[28] shows an excellent agreement if the calculated values are scaled by 0.957. In other words, B3LYP calculations overestimate vibrational frequecies by about 4%. The strongest peak for the quartet state of C_6^- appears at 1677 (1752) cm^{-1} if scaled by the same factor. For NC_4N^+ and CNC_3N^+, the strongest vibrational adsorptions occur at 2041 (2133) and 2014 (2105) cm^{-1}, respectively. There is a strong vibrational band of 2210 (2309) cm^{-1} for species CNC_3N^+. It is assumed that these numbers should be scaled by a similar factor.

Electronic Structures. The ground states of linear C_6^- and NC_4N^+ are described by the electron configuration ... $6\sigma_g^2\, 1\pi_u^4\, 6\sigma_u^2\, 7\sigma_g^2\, 1\pi_g^4\, 2\pi_u^3$. The relative energies of relevant occupied and unoccupied MOs are shown in Figure 2. In the dicyanoacetylene cations, the HOMO−LUMO gap is significantly larger than that of C_6^-. The large gap will result in fewer bands in the low-energy region for dicyanoacetylene cations compared with that for C_6^-. This is confirmed by MRD-CI calculations (*vide infra*). Notably, the ($6\sigma_u$, $7\sigma_g$) in NC_4N^+ is lower than $1\pi_u$, while CNC_3N^+ has an MO energy pattern similar to that of C_6^-. This suggests that there is a difference for bands due to ($6\sigma_u$, $7\sigma_g$) → $2\pi_u$ excitations between C_6^- and NC_4N^+, while the spectroscopic features of C_6^- and CNC_3N^+ may be more similar. Since electron correlation plays an important role in

TABLE 1: Vibrational Frequencies (cm^{-1}) of Linear C_6^-, NC_4N^+, and CNC_3N^+

	$\upsilon_1(\sigma_g^+)$	$\upsilon_2(\sigma_g^+)$	$\upsilon_3(\sigma_g^+)$	$\upsilon_4(\sigma_u^+)$	$\upsilon_5(\sigma_u^+)$	$\upsilon_6(\pi_g)$	$\upsilon_7(\pi_g)$	$\upsilon_8(\pi_u)$	$\upsilon_9(\pi_u)$
C_6^-									
X $^2\Pi_u$	2180	1854	653	2026	1213	607	258	439	121
scaled[a]	2086	1775	625	1939	1161	581	245	420	116
expt.[b]	2086	1775	634	1937					
$^4\Pi_g$	2141	1472	641	1752	1121	460	250	388	94
NC_4N^+									
X $^2\Pi_u$	2312	2033	632	2133	1239	568	266	477	108
CNC_3N^+									
X $^2\Pi$	2309	2105	1937	1300	658	533	427	216	108

[a] Calculated frequencies are scaled by a factor of 0.957. [b] Ref 28.

TABLE 2: Vertical Transition Energies and Oscillator Strength for the Doublet System of Linear C_6^- [a]

state	ΔE_e/eV	transition	f
X $^2\Pi_u$	0.00	...$2\pi_u^3$	
1 $^2\Sigma_g^+$	1.29(1.16)[b]	$7\sigma_g \rightarrow 2\pi_u$	0.0032
1 $^2\Sigma_u^+$	1.32	$6\sigma_u \rightarrow 2\pi_u$	0.0
1 $^2\Pi_g$	1.98(2.04)	$1\pi_g \rightarrow 2\pi_u$	0.3137
2 $^2\Pi_g$	2.84(2.79)	$2\pi_u \rightarrow 4\pi_g$	0.0096
1 $^2\Phi_g$	3.16	$2\pi_u \rightarrow 4\pi_g$	0.0
3 $^2\Pi_g$	3.57	$2\pi_u \rightarrow 4\pi_g$	0.0021
2 $^2\Pi_u$	4.19	$1\pi_u \rightarrow 2\pi_u$	0.0
1 $^2\Sigma_g^-$	4.76	$2\pi_u \rightarrow 8\sigma_g$	0.0
4 $^2\Pi_g$	4.87	$2\pi_u \rightarrow 2\pi_g$	0.0216
3 $^2\Pi_u$	4.80	$2\pi_u \rightarrow 3\pi_u$	0.0
1 $^2\Sigma_u^-$	4.85	$2\pi_u \rightarrow 7\sigma_u$	0.0
1 $^2\Delta_g$	5.08	$2\pi_u \rightarrow 8\sigma_g$	0.0
1 $^2\Delta_u$	5.12	$2\pi_u \rightarrow 7\sigma_u$	0.0
2 $^2\Phi_g$	5.15	$2\pi_u \rightarrow 2\pi_g$	0.0
1 $^2\Phi_u$	5.14	$2\pi_u \rightarrow 3\pi_u$	0.0
2 $^2\Sigma_u^+$	5.31	$2\pi_u \rightarrow 7\sigma_u$	0.0
2 $^2\Sigma_g^+$	5.32	$2\pi_u \rightarrow 8\sigma_g$	0.0
4 $^2\Pi_u$	5.45	$2\pi_u \rightarrow 3\pi_u$	0.0
2 $^2\Sigma_g^-$	5.59	$2\pi_u \rightarrow 9\sigma g$	0.0
2 $^2\Sigma_u^-$	5.60	$2\pi_u \rightarrow 8\sigma_u$	0.0
2 $^2\Delta_u$	5.86	$2\pi_u \rightarrow 8\sigma_u$	0.0
2 $^2\Delta_g$	5.82	$2\pi_u \rightarrow 9\sigma g$	0.0
3 $^2\Sigma_u^+$	6.03	$2\pi_u \rightarrow 8\sigma_u$	0.0

[a] For the degenerate states, the average value (obtained from the corresponding different irreducible representations) is listed. Among $^2\Pi_g$ states, only states up to $4^2\Pi_g$ are computed. [b] Experimental values.

TABLE 3: Vertical Transition Energies and Oscillator Strength for the Quartet System of Linear C_6^-

state	ΔE_e/eV	transition	f [a]
1 $^4\Pi_g$	0.00[b]	...$2\pi_u 2\pi_g$	
1 $^4\Sigma_u^+$	1.11	$7\sigma_g \rightarrow 2\pi_u$	0.0015
1 $^4\Sigma_g^+$	1.15	$6\sigma_u \rightarrow 2\pi_u$	0.0
1 $^4\Sigma_u^-$	1.69	$7\sigma_g \rightarrow 2\pi_u$	0.0037
1 $^4\Sigma_g^-$	1.72	$6\sigma_u \rightarrow 2\pi_u$	0.0
1 $^4\Delta_u$	1.81	$7\sigma_g \rightarrow 2\pi_u$	0.0031
1 $^4\Pi_u$	1.84	$1\pi_g \rightarrow 2\,\pi_u$	0.0248
		$2\pi_u \rightarrow 2\pi_g$	
1 $^4\Delta_g$	1.85	$6\sigma_u \rightarrow 2\pi_u$	0.0
2 $^4\Pi_u$	2.11	$1\pi_g \rightarrow 2\pi_u$	0.0288
		$2\pi_u \rightarrow 2\pi_g$	
2 $^4\Sigma_u^-$	2.21	$2\pi_g \rightarrow 7\sigma_u$	0.0068
1 $^4\Phi_u$	2.32	$1\pi_g \rightarrow 2\pi_u$	0.0
3 $^4\Pi_u$	2.39	$2\pi_g \rightarrow 3\pi_u$	0.0125
2 $^4\Sigma_g^-$	2.42	$2\pi_g \rightarrow 8\sigma_g$	0.0
3 $^4\Pi_u$	2.68	$1\pi_g \rightarrow 2\pi_u$	0.0049
2 $^4\Pi_g$	2.74	$2\pi_g \rightarrow 3\pi_u$	0.0
3 $^4\Sigma_u^-$	3.02	$2\pi_g \rightarrow 8\sigma_u$	0.0016
3 $^4\Sigma_g^-$	3.17	$2\pi_g \rightarrow 9\sigma_g$	0.0
3 $^4\Pi_g$	3.74	$2\pi_g \rightarrow 4\pi_g$	0.0
4 $^4\Sigma_g^-$	3.75	$2\pi_g \rightarrow 10\sigma_g$	0.0
3 $^4\Delta_u$	4.46	$2\pi_u \rightarrow 8\sigma_g$	0.0
3 $^4\Delta_g$	4.48	$2\pi_u \rightarrow 7\sigma_u$	0.0
2 $^4\Sigma_u^+$	4.50	$2\pi_u \rightarrow 8\sigma_g$	0.0
2 $^4\Sigma_g^+$	4.52	$2\pi_u \rightarrow 7\sigma_u$	0.0
4 $^4\Pi_g$	4.54	$2\pi_u \rightarrow 3\pi_u$	0.0
1 $^4\Phi_g$	4.74	$2\pi_u \rightarrow 3\pi_u$	0.0

[a] The f values are always given for one component of the degenerate states. [b] 1 $^4\Pi_g$ is calculated to be 2.50 eV above the X $^2\Pi_u$ state.

determining properties of the gound and the excited states for the carbon chains with the extended π-conjugation interaction, these MO energy patterns displayed in Figure 2 may be used only as a qualitative guide to the electronic structure and spectroscopic properties of the excited states.

Energies of Doublet and Quartet States of C_6^-. Calculated vertical excitation energies (ΔE_e), corresponding oscillator strengths (f), and the configuration character for the doublet and quartet states of C_6^- are presented in Tables 2 and 3. MRD-CI calculations predict that the lowest quartet state 1 $^4\Pi_g$ lies 2.50 eV above the ground-state X $^2\Pi_u$ at CCSD optimized geometries.

For the doublet system, the $7\sigma_g \rightarrow 2\pi_u$ excitation leads to the lowest transition of X $^2\Pi_u \rightarrow 1\ ^2\Sigma_g^+$, with a vertical transition energy of 1.29 eV ($f = 0.0032$). This value agrees reasonably with the observed band[17] at 1.16 eV. The next excited state 1 $^2\Sigma_u^+$ lies very close to the 1 $^2\Sigma_g^+$, as expected because $7\sigma_g$ and $6\sigma_u$ are energetically very close; transition from the ground state to this state is forbidden by the dipole-selection rule, however. A strong X $^2\Pi_u \rightarrow 1\ ^2\Pi_g$ band due to the $1\pi_g \rightarrow 2\pi_u$ excitation is calculated at 1.98 eV with $f = 0.314$. This absorption band has been observed at 2.04 eV in neon matrix.[16] The $2\pi_u \rightarrow 4\pi_g$ electronic excitation results in the excited states 2 $^2\Pi_g$, 3 $^2\Pi_g$, and 1 $^2\Phi_g$ at 2.84, 3.16, and 3.57 eV, respectively, where $4\pi_g$ from the state-averaged CASSCF optimization is characterized as valence-type MO. The corresponding oscillator strengths are relatively small, however. The calculated band at 2.84 eV matches well with the observed adsorption at 2.79 eV.[17]

In previous gas-phase spectra, this band was assigned to X $^2\Pi_u \rightarrow 3\ ^2\Pi_g$, and a lower peak at 2.49 eV was suggested to be the X $^2\Pi_u \rightarrow 2\ ^2\Pi_g$ band system.[17] However, our calculations for the doublet series have not found a transition around 2.49 eV. Further, we have performed state-averaged CASSCF/CASPT2 calculations to estimate the effect of theoretical treatment on the transition energy. Again, CASPT2 calculations predict that electronic transitions to 1 $^2\Pi_g$, 2 $^2\Pi_g$, and 3 $^2\Phi_g$ appear at 1.94, 2.85, and 3.05 eV, respectively. Interestingly, the term energy of the doublet−quartet transition X $^2\Pi_u \rightarrow 1\ ^4\Pi_g$ is 2.50 eV. This doublet−quartet electronic transition is formally spin-forbidden, but may be possible by spin−orbit interactions, and could account for the observed feature at 2.49 eV. The highest state resulting from excitations into a valence orbital is 2 $^2\Pi_u$ ($1\pi_u \rightarrow 2\pi_u$), calculated at 4.19 eV, but the corresponding transition is forbidden by dipole-selection rules.

In the higher-energy region, all transitions are from HOMO into the relative diffuse orbtials $2\pi_g$, $3\pi_u$, $7\sigma_u$, $8\sigma_u$, $8\sigma_g$, $9\sigma_g$, which are composed primarily from Rydberg-like functions. It

TABLE 4: Vertical Transition Energies and Oscillator Strength for the Doublet System of Linear NC_4N^+

state	ΔE_e/eV	transition	f [a]
X $^2\Pi_u$	0.0	...$2\pi_u^3$	
A $^2\Pi_g$	2.14(2.07)[b]	$1\pi_g \rightarrow 2\pi_u$	0.1078
B $^2\Sigma_g^+$	2.22(2.16)[c]	$7\sigma_g \rightarrow 2\pi_u$	0.0015
C $^2\Sigma_u^+$	2.27(2.32)[c]	$6\sigma_u \rightarrow 2\pi_u$	0.0
D $^2\Pi_u$	3.32(3.16)[c]	$1\pi_u \rightarrow 2\pi_u$	0.0
2 $^2\Pi_g$	3.69	$2\pi_u \rightarrow 2\pi_g$	0.0183
1 $^2\Phi_g$	4.17	$2\pi_u \rightarrow 2\pi_g$	0.0
3 $^2\Pi_g$	4.93	$2\pi_u \rightarrow 2\pi_g$	0.0153
1 $^2\Phi_u$	5.56	$1\pi_g \rightarrow 2\pi_g$	0.0
2 $^2\Sigma_u^+$	6.09	$7\sigma_g \rightarrow 2\pi_g$	0.0

[a] All f values are listed for one component of degenerate states. [b] Experimental value. [c] Deduced from ionization energy differences relative to the A $^2\Pi_g$ of the photoelectron spectrum of dicyanoacetylene.

TABLE 5: Vertical Transition Energies and Oscillator Strength for the Doublet System of Linear CNC_3N^+

state	ΔE_e/eV	transition	f
X $^2\Pi$	0.00	...$3\pi^3$	
1 $^2\Sigma^+$	0.95	$13\sigma \rightarrow 3\pi$	0.0004
2 $^2\Sigma^+$	2.23	$12\sigma \rightarrow 3\pi$	0.0008
2 $^2\Pi$	2.65	$2\pi \rightarrow 3\pi$	0.0749
3 $^2\Pi$	3.69	$3\pi \rightarrow 4\pi$	0.0071
1 $^2\Phi$	4.20	$3\pi \rightarrow 4\pi$	0.0
1 $^2\Sigma^-$	4.45	$13\sigma \rightarrow 4\pi$	0.0001
3 $^2\Sigma^+$	4.52	$13\sigma \rightarrow 4\pi$	0.0001
1 $^2\Delta$	4.65[a]	$13\sigma \rightarrow 4\pi$	0.012
2 $^2\Delta$	5.70	$13\sigma \rightarrow 4\pi$	0.0189

[a] For the degenerate states, the average value (obtained from the corresponding different irreducible representations) is listed. Π states are calculated only up to 3 $^2\Pi$.

is not clear whether these states can be considered as resonance-like states which couple to the continuum or whether occupation of the upper diffuse orbital is simply an indication that the preferred state would be C_6 + e. The energy of these states is above that of neutral C_6. Only the transition X $^2\Pi_u \rightarrow 4\ ^2\Pi_g$ at 4.87 shows a large oscillator strength.

In the quartet series, the lowest electronic transition 1 $^4\Pi_g \rightarrow 1\ ^4\Sigma_u^+$ occurs at 1.11 eV due to the $7\sigma_g \rightarrow 2\pi_u$ electronic excitation. The other excited states 1 $^4\Sigma_u^-$ and 1 $^4\Delta_u$ resulting from the same electronic configuration are calculated at 1.69 and 1.81 eV above the lowest quartet state, respectively, with small ($f = 0.003$) transition probability. Next lowest 1 $^4\Sigma_g^+$ state due to the $6\sigma_u \rightarrow 2\pi_u$ intravalence excitation is 1.15 eV above the 1 $^4\Pi_g$ state. The $6\sigma_u \rightarrow 2\pi_u$ excitation also accounts for the excited states 1 $^4\Delta_g$ and 1 $^4\Sigma_g^-$, in the range between 1.70 and 2.0 eV. Corresponding transitions are symmetry-forbidden. The $1\pi_g \rightarrow 2\pi_u$ and $2\pi_u \rightarrow 2\pi_g$ excitations may result in the excited states 1 $^4\Pi_u$ and 2$^4\Pi_u$, respectively, calculated at 1.84 and 2.11 eV with oscillator strengths of 0.026. The $1\pi_g \rightarrow 2\pi_u$ excitation is also responsible for the bands of 1 $^4\Pi_g \rightarrow 1\ ^4\Phi_u$ and 1 $^4\Pi_g \rightarrow 2\ ^4\Phi_u$ at 2.32 and 2.68 eV. Here, $2\pi_g$ of the quartet state, obtained by separate CASSCF optimization, is the valence-type MO, in contrast to the doublet state, in which $2\pi_g$ is essentially a Rydberg-like function.

Energies of Doublet States of NC_4N^+ and CNC_3N^+. The vertical transition energies and oscillator strengths for the doublet system of NC_4N^+ and CNC_3N^+ are collected in Tables 4 and 5. All low-lying excitations arise from transitions into the partially filled $2\pi_u$. The lowest excited state for the NC_4N^+ isomer is the A$^2\Pi_g$. The MRD-CI calculation show a strong transition to this state at 2.14 eV with $f = 0.11$. In previous laser-indued fluorescence spectra,[19] the band system at 2.07 eV

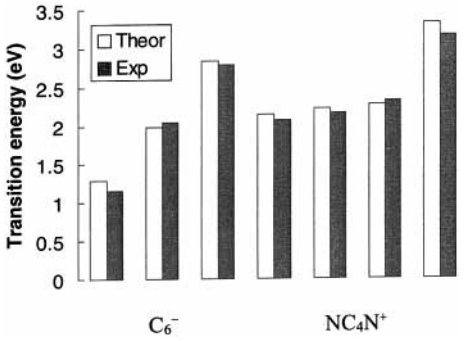

Figure 3. A comparison of calculated and observed transition energies of C_6^- and NC_4N^+.

was assigned to this transition. On the basis of the X $^2\Pi_u \rightarrow$ A $^2\Pi_g$ band system, the photoelectron spectrum[19] of dicyanoacetylene suggests that the excited states B $^2\Sigma_g^+$, C $^2\Sigma_u^+$, and D $^2\Pi_u$ states are placed at 2.16, 2.32, and 3.16 eV, respectively, above the ground-state X $^2\Pi_u$. It is seen that the calculated energies are in good agreement with the photoelectron−photon coincidence studies.[19] Similar to the low-lying states 1 $^2\Sigma_g^+$ and 1 $^2\Sigma_u^+$ of C_6^-, the excited states B $^2\Sigma_g^+$ and C $^2\Sigma_u^+$ are nearly degenerate. The $2\pi_u \rightarrow 2\pi_g$ excitation leads to excited states 2 $^2\Pi_g$, 1 $^2\Phi_g$, and 3 $^2\Pi_g$, which were calculated to be at 3.69, 4.17, and 4.93 eV, respectively.

The first transition X $^2\Pi \rightarrow 1\ ^2\Sigma^+$ due to the $13\sigma \rightarrow 3\pi$ excitation for CNC_3N^+ is placed at 0.95 eV with $f = 0.0004$. The $12\sigma \rightarrow 3\pi$ excitation gives rise to the 2 $^2\Sigma^+$ excited state, which is 2.23 eV above the ground X $^2\Pi$state. Both states correspond to the close-lying states $^2\Sigma_g^+$ and $^2\Sigma_u^+$ in C_6^- and NC_4N^+. In CNC_3N^+, these states are able to mix because of the lack of inversion symmetry, and this mixing leads to the relatively large splitting between these two $^2\Sigma^+$ states in CNC_3N^+. A strong X$^2\Pi \rightarrow 1\ ^2\Pi$ band was found at 2.65 eV with $f = 0.075$ due to the $2\pi \rightarrow 3\pi$ excitation. The X $^2\Pi \rightarrow 3\ ^2\Pi$ transition due to $3\pi \rightarrow 4\pi$ excitation is calculated at 3.69 eV with $f = 0.0071$. Among higher excitations, strong absorptions X $^2\Pi \rightarrow 1\ ^2\Delta$ and X $^2\Pi \rightarrow 2\ ^2\Delta$ appear at 4.65 and 5.70 eV, respectively.

Conclusions

An *ab initio* study of the electronic spectra of isoelectronic species C_6^-, NC_4N^+, and CNC_3N^+ has been carried out. Assignments to observed transitions for C_6^- and NC_4N^+ in the gas-phase spectroscopy have been made. All strong transitions for the doublet species arise from intravalence $\pi \rightarrow \pi$ excitations. These strongest $^2\Pi \rightarrow {}^2\Pi$ electronic absorptions of species C_6^-, NC_4N^+, and CNC_3N^+ are calculated at 1.98, 2.14, and 2.65 eV, respectively. Present calculations suggest that the band feature at 2.49 eV in the gas-phase spectra of C_6^- may be assigned to the X $^2\Pi_u \rightarrow 1^4\Pi_g$ transition or the concomitant presence of certain species. The X $^2\Pi_u \rightarrow 2\ ^2\Pi_g$ transition, which was assigned to the 2.49 eV band in previous experimental study, is calculated at 2.84 eV. Even though C_6^- and NC_4N^+ have similar X $^2\Pi_u \rightarrow 1\ ^2\Pi_g$ band systems, the transitions to the $^2\Sigma_g^+$ and $^2\Sigma_u^+$ are at considerably higher energy in NC_4N^+; this difference can be ascribed to the different energy of σ and $1\pi_u$ MOs in the two systems. A comparison of calculated results with experimental data in Figure 3 shows an excellent agreement between theoretical predictions and observed spectra. Linear C_6^- and NC_4N^+ chains are determined to be the most stable forms at all levels of theory considered in the present work for C_6^- and dicyanolyacetylene cations.

Acknowledgment. Z.C. thanks the Alexander von Humboldt Foundation for financial support during his stay in Universität Bonn. He is grateful to Dr. M. Mühlhäuser and Dr. M. Hanrath for support in using the DIESEL-CI program.

References and Notes

(1) Maier, J. P. *Chem. Soc. Rev.* **1997**, *26*, 21.
(2) Fulara, J.; Lessen, D.; Freivogel, P.; Maier, J. P. *Nature* **1993**, *366*, 439.
(3) Freivogel, P.; Fulara, J.; Maier, J. P. *Astrophys. J.* **1994**, *431*, L151.
(4) Maier, J. P. *Nature* **1994**, *370*, 423.
(5) Bernath, P. F.; Hinkle, K. H.; Keady, J. J. *Science* **1989**, *244*, 562.
(6) Kolbuszewski, M. *J. Chem. Phys.* **1995**, *102*, 3679.
(7) Grutter, M.; Wyss, M.; Riaplov, E.; Maier, J. P.; Peyerimhoff, S. D.; Hanrath, M. *J. Chem. Phys.* **1999**, *111*, 7397.
(8) Forney, D.; Grutter, M. Freivogel, P.; Maier, J. P. *J. Phys. Chem. A* **1997**, *101*, 5292.
(9) Douglas, A. E. *Nature* **1977**, *269*, 130.
(10) Bell, M. B.; Feldman, P. A.; Matthews, H. E. *Astron. Astrophys.* **1981**, *101*, L13.
(11) Orden, A. V.; Saykally, R. J. *Chem. Rev.* **1998**, *98*, 213.
(12) Weltner, W., Jr.; Van Zee, R. J. *Chem. Rev.* **1989**, *89*, 1713.
(13) Schmatz, S.; Botschwina, P. *Chem. Phys. Lett.* **1995**, *235*, 5.
(14) Adamowiz, L. *Chem. Phys. Lett.* **1991**, *182*, 45.
(15) Watts, J. D.; Bartlett, R. J. *J. Chem. Phys.* **1992**, *97*, 3445.
(16) Forney, D.; Fulara, J.; Freivogel, P.; Jakobi, M.; Lessen, D.; Maier, J. P. *J. Chem. Phys.* **1995**, *103*, 48.
(17) Freivogel, P.; Grutter, M.; Forney, D.; Maier, J. P. *J. Chem. Phys.* **1997**, *107*, 22.
(18) Feher, M.; Maier, J. P. *Chem. Phys. Lett.* **1994**, *227*, 371.
(19) Maier, J. P.; Misev, L.; Thommen, F. *J. Phys. Chem.* **1982**, *86*, 514.
(20) Poirier, P.; Kari, R.; Csizmadia, L. G. *Handbook of Gaussian Basis Sets*; Elsevier: New York, 1985.
(21) Dunning, T. H., Jr.; Hay, Jeffrey, P. In *Methods of Electronic Structure Theory*; Schaefer, H. F., III, Ed.; Plenum: New York, 1977.
(22) Mclean, A. D.; Chandler, G. S. *J. Chem. Phys.* **1980**, *72*, 5639.
(23) Krishnan, R.; Blinkley, J. S.; Seeger, R.; Pople, J. A. *J. Chem. Phys.* **1980**, *72*, 650.
(24) (a) Buenker, R. J.; Peyerimhoff, S. D. *Theor. Chim. Acta* **1974**, *35*, 33. (b) Buenker, R. J.; Peyerimhoff, S. D. *Theor. Chim. Acta* **1975**, *39*, 217. (c) Buenker, R. J.; Peyerimhoff, S. D. Butscher, W. *Mol. Phys.* **1978**, *35*, 771.
(25) Frisch, M. J.; Trucks, G. W.; Schlegel, H. B.; Gill, P. M. W.; Johnson, B. G.; Robb, M. A.; Cheeseman, J. R.; Keith, T.; Petersson, G. A.; Montgomery, J. A.; Raghavachari, K.; Al-Laham, M. A.; Zakrzewski, V. G.; Ortiz, J. V.; Foresman, J. B.; Peng, C. Y.; Ayala, P. Y.; Chen, W.; Wong, M. W.; Andres, J. L.; Replogle, E. S.; Gomperts, R.; Martin, R. L.; Fox, D. J.; Binkley, J. S.; Defrees, D. J.; Baker, J.; Stewart, J. P.; Head-Gordon, M.; Gonzalez, C.; Pople, J. A. *Gaussian 94*, Revision B.3; Gaussian Inc.: Pittsburgh, PA, 1994.
(26) Andersson, K.; Blomberg, M. R. A.; Fülscher, M. P.; Karlström, G.; Lindh, R.; Malmqvist, P.-Å.; Neogrády, P.; Olsen, P.; Roos, B. O.; Sadlej, A. J.; Schütz, M.; Seijo, L.; Serranp-Andrés, L.; Siegbahn, P. E.; Widmark, P.-O. *MOLCAS*, Version 4; Lund University: Lund, Sweden, 1997.
(27) Hanranth, M.; Engels, B. *Chem. Phys.* **1997**, *225*, 167.
(28) Szczepanski, J.; Auerbach, E.; Vala, M. *J. Phys. Chem.* A **1997**, *101*, 9296.